JOURNAL OF Applied Polymer SCIENCE

Enthalpy Relaxation of Photopolymerized Multilayered Thiol-Ene Films

Junghwan Shin,[1,2] Sergei Nazarenko,[1] Charles E. Hoyle[1]

[1]School of Polymers and High Performance Materials, University of Southern Mississippi, Hattiesburg, Mississippi 39406

[2]Manufacturing Technology Center, Samsung Electronics, Suwon, Gyunggi-do, South Korea 443-742

Correspondence to: J. Shin (E-mail: junghwanshin@hotmail.com)

ABSTRACT: Multilayered thiol-ene network films with two and three different components were fabricated by spin coating and photopolymerization. The distinctive glass transition temperatures of each layer component were observed at corresponding glass transition regions of each bulk sample. Sub-T_g aging of 10-, 21-, and 32-layered thiol-ene films was investigated in terms of enthalpy relaxation. Enthalpy relaxation of each layer component occurred independently and presented the characteristic time and temperature dependency. Overlapped unsymmetrical bell-shaped enthalpy relaxation distribution having peak maximum at T_g-10°C of each layer component was observed, resulting in broad distribution of enthalpy relaxation over wide temperature range. In addition, enthalpy relaxation of each layer component in the multilayered thiol-ene films was significantly accelerated comparing to that of bulk thiol-ene samples. Dynamic mechanical thermal properties of multilayered thiol-ene films also showed two and three separated glass transition temperature. However, for 32-layered thiol-ene film consisting of three different layer components, glass transition and damping region are overlapped and the width is extended more than 100°C. © 2012 Wiley Periodicals, Inc. J. Appl. Polym. Sci. 000: 000–000, 2012

KEYWORDS: glass transition; photopolymerization; thermal properties; properties and characterization; structure–property relations

Received 7 July 2012; accepted 7 August 2012; published online

DOI: 10.1002/app.38443

INTRODUCTION

Photopolymerized thiol-ene networks have attracted much interest in academia as well as industries due to the unique reaction mechanism and chemical structure.[1–13] The kinetics of thiol-ene reactions following free-radical step reactions and resultant uniform networks structure have been extensively studied by Bowman and Hoyle since 2000.[6–13] Uniform and highly dense network structure results in narrow glass transition temperature (FWHM < 20°C) and very high damping factor (tan δ < 1.6) due to probably narrow distribution of relaxation times.[1,14] Recently, the physical importance of the uniformity of thiol-ene networks has been reported by correlating chemical structure of thiol-ene networks and sub-T_g aging in terms of enthalpy relaxation.[15,16] The overall relaxation is significantly affected by chemical structural parameters such as network uniformity, crosslink density, rigidity, bulky side groups, and hydrogen bonding. It is well known that apparent glass transition temperature and physical/mechanical properties of polymer materials can be potentially changed during the sub-T_g aging. In most cases, maximum enthalpy relaxation rate is observed at T_g-10°C that resulted by the competition between thermodynamic driving force and molecular mobility.[15] As photopolymerized thiol-ene based materials mostly have T_g near room temperature, the considerable property changes by sub-T_g aging are expected. Thus, it has been reported that the overall rate (β_H) and extent of enthalpy relaxation (δ_H) can be successfully restricted by chemical and physical modification of the thiol-ene network structure.[16]

Polymer thin films are widely being used as a membrane for gas separation and food packaging. Also, recently their applications are expanding over many applications with the increasing demand of miniaturizing electronic devices.[17–20] It is known that as thickness decreases, the physical properties of very thin polymer films appear to be different with what is observed in the bulk.[21–24] Special attention has been paid to study glass transition (T_g) behavior in confined thin films where the T_g is correlated to the chain mobility and interfacial interaction with substrate.[24,25] In the case of polymer films having weak interaction with the substrate, T_g usually decreases with decreasing film thickness.[21,22] If such a thin film is removed from the substrate, the resultant free-standing film has much different T_g than the film attached to the substrate.[23] On the contrary, an increase of T_g with decreasing film thickness has been shown for a PMMA (poly(methyl-methacrylate)) thin film on a hydrophilic-modified substrate where there is strong interaction between the polymer thin film and the substrate.[24,25] Therefore, it is concluded that, at least for linear, noncrosslinked or network polymers, the nature of the substrate-film interface is a

Applied Polymer SCIENCE

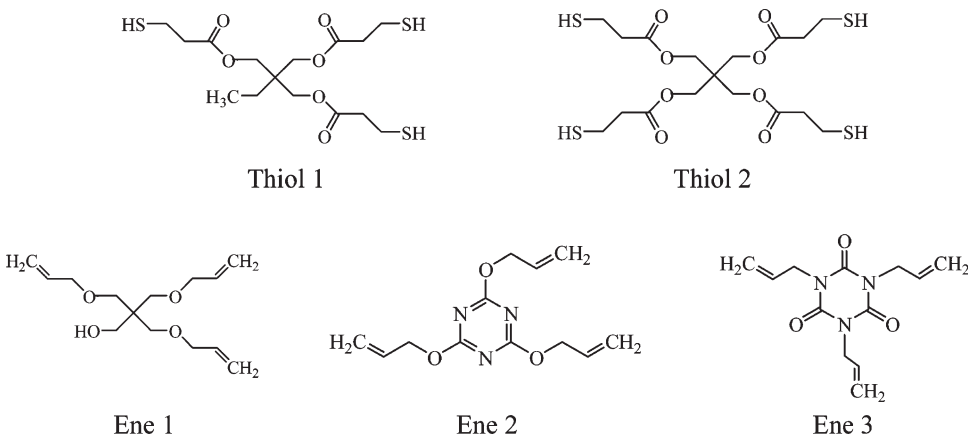

Figure 1. The chemical structure of thiol and ene monomers.

critical factor affecting the thermal properties of polymer thin films. Especially, it can be speculated that the substrate-film interface will also affect relaxation processes upon physical aging. Interestingly, several recent reports have shown that the accelerated physical aging of thin films formed from linear polymers result in drastic changes of physical properties on very short time scales.[18–20,26–28] Huang et al. observed more rapid increase in refractive index of thin films than that of thick films for linear polymers.[26] It has also reported that gas permeability of polymer thin films significantly decrease as a function of time, which has been correlated to physical aging.[19,20,26–28] Because gas permeation of polymeric materials is directly related to free volume, the accelerated physical aging for polymer thin films seems to result in the rapid free volume changes.

Multilayered films of different polymers are commonly used in many applications such as gas barriers for food packaging and anti-reflective optical coatings.[29–31] These multilayered films consist of a few to thousands layers with two or more different polymers. Each polymer has different physical properties and sensitivity to environment, i.e., environment changes such as temperature and humidity, so that the responses to environmental change are individual. Thus, it is important to characterize and understand the physical and mechanical properties of each layer within the multilayered films. For instance, if each polymer or layer is actually phase separated without any chemical bonding, they will undergo sub-T_g aging at different rate for a specific set of annealing conditions due to their different molecular parameters, such as chain rigidity and cross-link density.

In this article, 10-, 21-, and 32-layered thiol-ene photo-polymerized films were fabricated with two and three different chemical compositions, respectively, by spin coating and evaluated in terms of sub-T_g aging monitored by enthalpy relaxation. The extent and rate of enthalpy relaxation of multilayered thiol-ene network films were investigated and compared with bulk samples of each composition. In addition, layering thiol-ene films, which have high uniform dense network resulting in glass transition occurring at narrow temperature region, provided a good venue as a damping material through the wide temperature range of loss modulus and tan δ.

EXPERIMENTAL

Materials

Thiols (Trimethylolpropane tris(3-mercaptopropionate) (Thiol 1) and pentaerythritol tetra(3-mercaptopropionate) (Thiol 2)) and ene monomers (allyl pentaerythritol (Ene 1), 2,4,6-triallyloxy-1,3,5-triazine (Ene 2), and 1,3,5-triallyl-1,3,5-triazine-2,4,6(1H,3H,5H)-trione (Ene 3)) were obtained from Bruno Bock Thio-Chemicals-S and Perstorp Specialty Chemicals, respectively (Figure 1). The photoinitiator, 2,2-dimethoxy 2-phenyl acetophenone (DMPA), was obtained from Ciba Specialty Chemicals and directly used without purification.

Preparation of Multilayered Thiol-ene Films

Each layer has different glass transition temperature by the combination of different thiol and ene monomers that have different functionality and rigidity (Thiol 1-Ene 1 : $T_g = -14°C$, Thiol 2-Ene 2 : $T_g = 10°C$, and Thiol 2-Ene 3 : $T_g = 45°C$). Thiols and enes for each layer were mixed with 1 wt % of photo-initiator (DMPA) and sonicated for 30 min in order to dissolve it. Multilayered thiol-ene network films were prepared by repeating spin coating and UV irradiation on the glass plate (2.5×2.5 cm^2). UV lamp was shuttered using an electrically automated optical shutter while each layer was spin-coated. Thickness of each layer was controlled by the spin rate and UV light was irradiated for 30 s with low pressure mercury lamp (254 nm, 0.1 mW/cm^2). Photopolymerized multilayered thiol-ene network films were postcured at 80°C, which is higher than T_g of all thiol-ene layer components, for 12 h in order to ensure full conversion of thiol-ene free-radical reaction and remove the possibility of unexpected chemical structural change during physical aging. Figure 2 illustrates a diagram for multilayered thiol-ene network films consisting of three types of thiol-ene network layers with three separate T_gs as well as physical aging behavior at specific temperature and time. Thickness of each layer and film was controlled by the amount of mixture and rpm of spin coater. Thickness of each layer was calculated with the weight, density of monomers, and area of glass plate when prepared and it was compared with SEM analysis after the completion of the postcuring. The difference of thickness between the value obtained by the calculation and actual measurement was less than 5%, which resulted by the shrinkage during

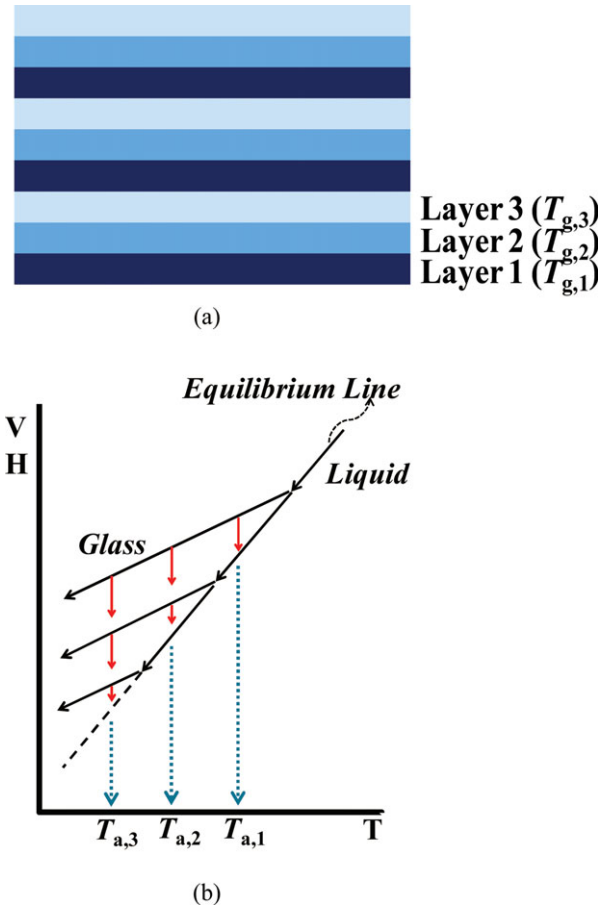

Figure 2. (a) Layer by layer structure thiol-ene network films with three different components, (b) diagram of physical aging of multilayered thiol-ene network films at three different annealing temperatures (T_a). [Color figure can be viewed in the online issue, which is available at wileyonlinelibrary.com.]

network formation. Two different sets of multilayered thiol-ene network films were prepared in this study. For the first set, 10-, 21-, and 32-layered thiol-ene network films were fabricated by alternating two layer components (Thiol 1-Ene 1 and Thiol 2-Ene 3) with the variation of overall thickness. 21- and 32-layered thiol-ene network films were made by combining 10-layered thiol-ene film (containing Thiol 1-Ene 2 and Thiol 2-Ene 3) with Thiol 1-Ene 1 and Thiol 2-Ene 3 monomer mixtures as adhesion layers. The average thicknesses of Thiol 1-Ene 1 and Thiol 2-Ene 3 were 47 and 43 μm, respectively. The overall thicknesses of 10-, 21-, and 32-layered thiol-ene network films were 450, 950, and 1430 μm, respectively, and the weight ratio of all three systems was about 55:45. The second set of sample was prepared by layering three different thiol-ene system (Thiol 1-Ene 1, Thiol 2-Ene 1, and Thiol 2-Ene 2) and the average thicknesses were 16, 20, and 17 μm, respectively. The number of each layer (9:10:13) and weight ratio (25:35:40) were determined based on the results reported in our previous study.[15] The heat capacity change at T_g (ΔC_p) on DSC heating scan is directly related to the overall rate and amount of enthalpy relaxation (the area of enthalpy relaxation peak). Also, the chemical structure of thiol and ene monomers, i.e., functionality and rigidity, has a significant effect on the enthalpy relaxation. Thus, 10-layered thiol-ene network film of the first set of thiol-ene network films was simply designed to show the distinct difference of enthalpy relaxation distribution of each composition at approximately the same weight ratio (55:45) by weight. 21- and 32-layered thiol-ene network films were additionally prepared in order to investigate the effect of number of layers with the same layer components on the enthalpy relaxation. For 32-layred thiol-ene network film of the second set, the number of layers and weight ratio were designed based on quantitative calculation using ΔC_p, resulting in the ratio of 9:10:13 by layers and 25:35:40 by weight. The overall thickness was 564 μm for 32-layered thiol-ene network film.

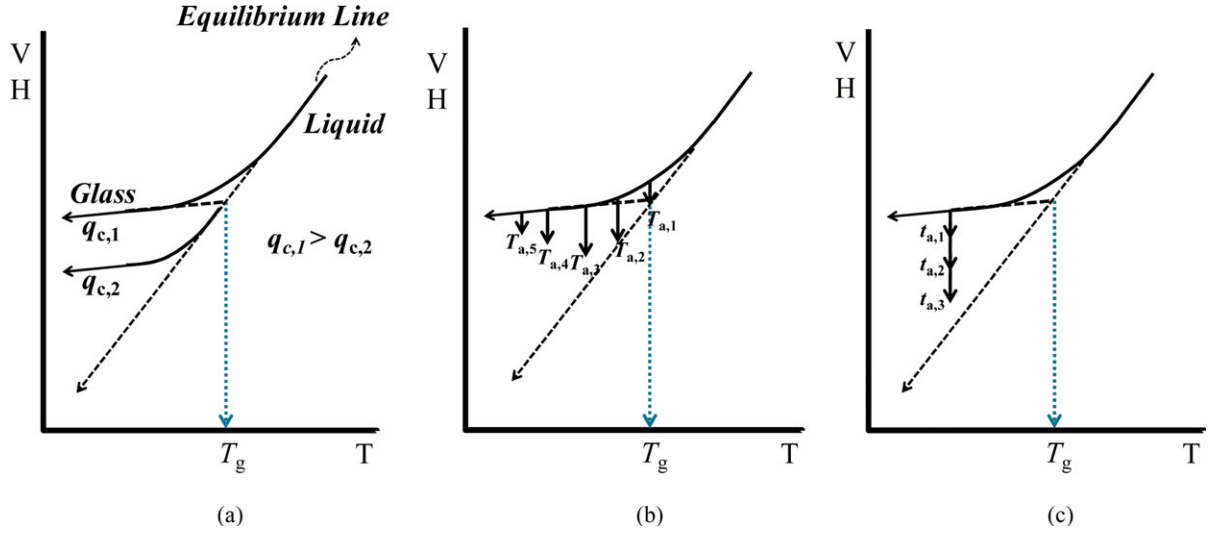

Figure 3. Physical aging behavior by different annealing methods; (a) Differential cooling rate (q_c: cooling rate), (b) Isochronal (annealing time, t_a = constant), and (c) Isothermal (annealing temperature, T_a = constant). [Color figure can be viewed in the online issue, which is available at wileyonlinelibrary.com.]

Applied Polymer SCIENCE

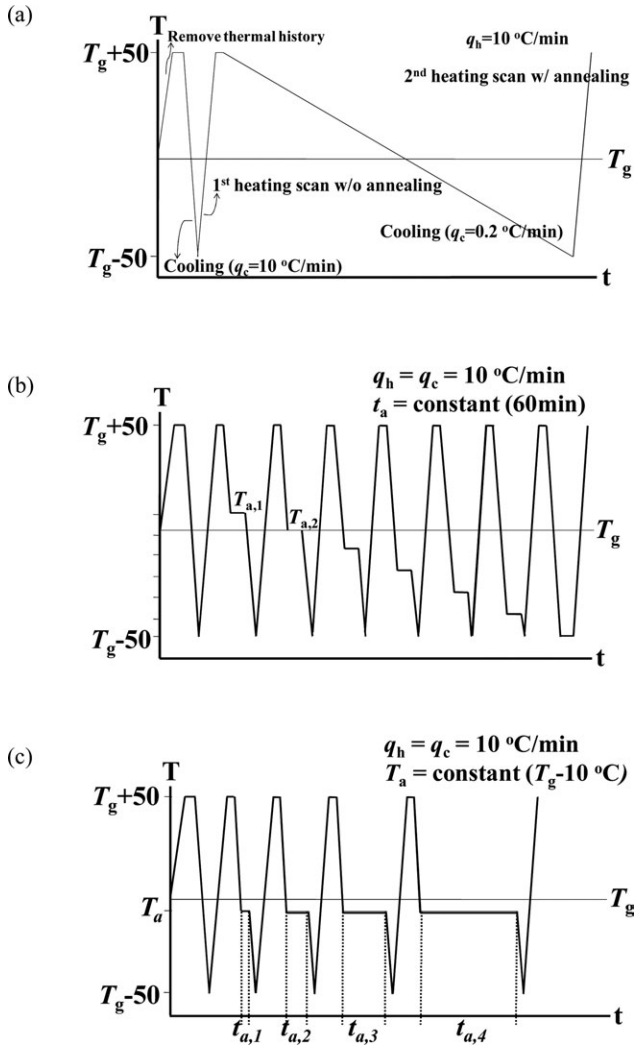

Figure 4. Three different experimental procedures for enthalpy relaxation; (a) Differential cooling rate, (b) Isochronal, and (c) Isothermal; q_c and q_h = cooling and heating rate, t_a = annealing time, T_a = annealing temperature.

Characterization

Glass transition temperatures and thermal properties were measured with a TA Q800 dynamic mechanical analyzer (DMA) from −80 to 200°C at a heating rate of 3°C/min and frequency of 1 Hz using tensile mode, and a TA Q1000 differential scanning calorimeter (DSC) from −60 to 120°C at a 10°C/min heating and cooling rate. TA Q1000 was set up with RCS 90 (Refrigerated Cooling System). A RCS 90 cooling head mounted on the DSC Q1000 furnace encases the DSC cell preventing frost building-up during operation. Three calibration steps (T_{zero} calibration, enthalpy constant calibration, and Temperature calibration) for the TA Q1000 were performed periodically. Detailed calibration protocol has been well described in a previous literature.[15,16]

Three different aging methods were used to characterize enthalpy relaxation of multilayered thiol-ene films as described in Figure 3 which showed time (isothermal) and temperature (isochronal) dependency of physical aging as well as different cooling rates potentially show the distribution of enthalpy relaxation (Figure 4). Special attention was paid to running the DSC to ensure the accuracy of the enthalpy relaxation measurement. For three different annealing methods described in Figure 3, the measurement was conducted twice and the sequence of annealing was reversed in the second running. Equivalent results were obtained in both cases, i.e., instrumental drift did not play a factor, and the results were reproducible despite the different order in obtaining the data sets. Furthermore, the heat flow and heat capacity of Thiol 1-Ene 1 sample without aging, as a standard, were measured after every calibration and time-sequence scan to ensure consistency. Finally, in order to remove sampling errors, the same DSC pans (samples) were used for all measurements. All experiments were carried out under nitrogen with a flow rate of 50 mL/min. Sample weights were 8.0 ± 1.0 mg to ensure sufficient sensitivity for heat capacity measurements. DSC scans were conducted over the temperature range of ±50°C from the highest and lowest glass transition temperature of multilayered thiol-ene films. Annealing temperature (T_a),

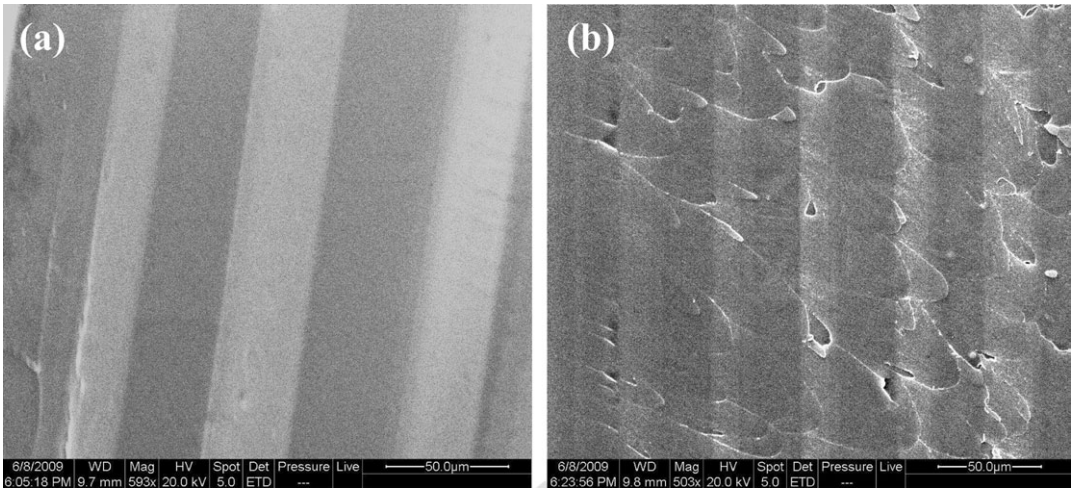

Figure 5. SEM images of fractured surface of (a) 10- (set 1, Thiol 1-Ene 1 and Thiol 2-Ene 3) and (b) 32-layered (set 2, Thiol 1-Ene 1, Thiol 2-Ene 2 and Thiol 2-Ene 3) thiol-ene network films.

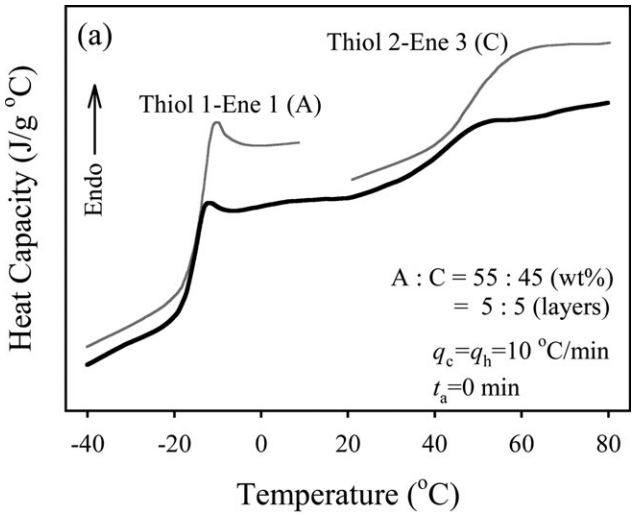

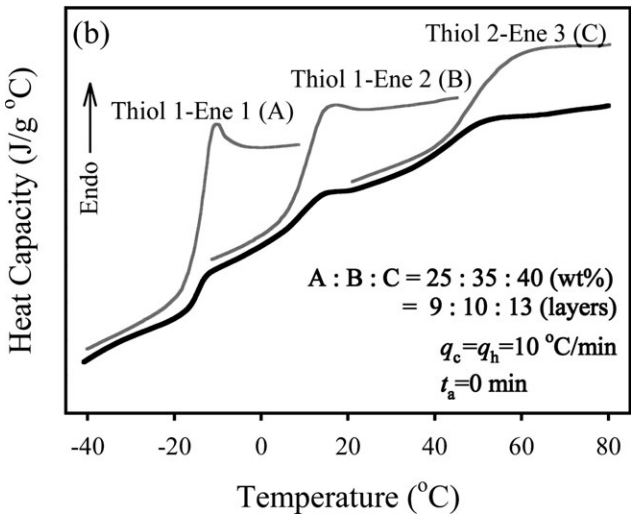

Figure 6. Thermal properties of (a) 10- (set 1, Thiol 1-Ene 1 and Thiol 2-Ene 3) and (b) 32-layered (set 2, Thiol 1-Ene 1, Thiol 2-Ene 2, and Thiol 2-Ene 3) thiol-ene network films.

annealing time (t_a), and cooling rate (q_c) were controlled to establish different annealing methods. Detailed descriptions of measurement techniques are described in mthe text.

The morphology of multilayered thiol-ene films was obtained using scanning electron microscopy (SEM) (Quanta 200 SEM) in the high-voltage mode. Multilayered thiol-ene films were quenched in liquid nitrogen and fractured followed by mounting on the SEM sample holders with epoxy. Samples were sputter-coated with a 5-nm gold layer using a Emitech K550X sputter coater to enhance the image quality.

RESULTS AND DISCUSSION

Morphology

In Figure 5, the SEM images of fractured surface of 10- (set 1) and 32-layered (set 2) thiol-ene films show that multilayered structure is well defined for both samples and the delamination between layers are not observed. Thickness of each layer for each sample is approximately consistent with the calculated average thickness, i.e. 43 ± 2 μm for 10-layered film (set 1) and 17 ± 2 μm for 32-layered film (set 2).

Thermal Properties

DSC thermograms and glass transition temperatures of 10- (set 1) and 32-layered (set 2) thiol-ene films and bulk samples of each layer composition were shown in Figure 6. Two and three distinctive separated T_gs were observed for 10-layered (a) and 32-layered films (b), respectively, corresponding glass transition temperature of each layer in bulk. It seems that adjacent layers does not affect much on chain mobility and thermal property each other because each layer has pretty great thickness (40 ± 2 μm for set 1 and 17 ± 2 μm for set 2) to exhibit its own T_g and no chemical and physical interaction between layers.

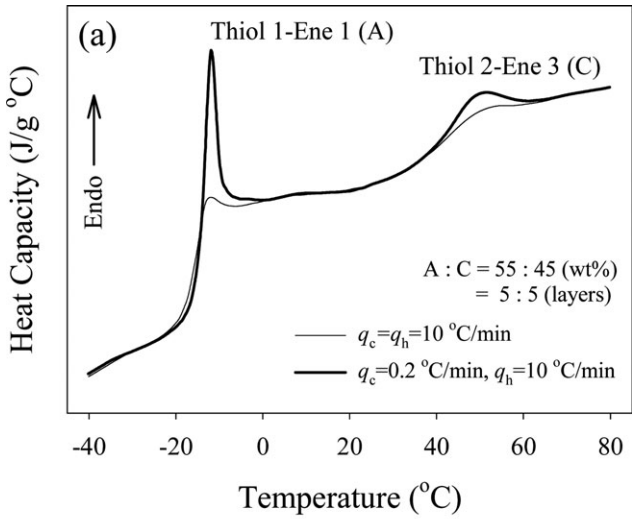

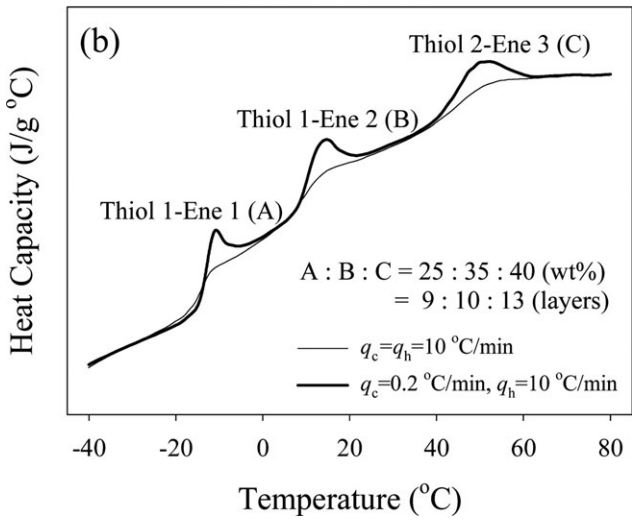

Figure 7. DSC heating scans (q_h =10°C/min) of (a) 10- (set 1, Thiol 1-Ene 1 and Thiol 2-Ene 3) and (b) 32-layered (set 2, Thiol 1-Ene 1, Thiol 2-Ene 2, and Thiol 2-Ene 3) thiol-ene network films after different cooling rate (q_c = 10 and 0.2°C/min).

Applied Polymer SCIENCE

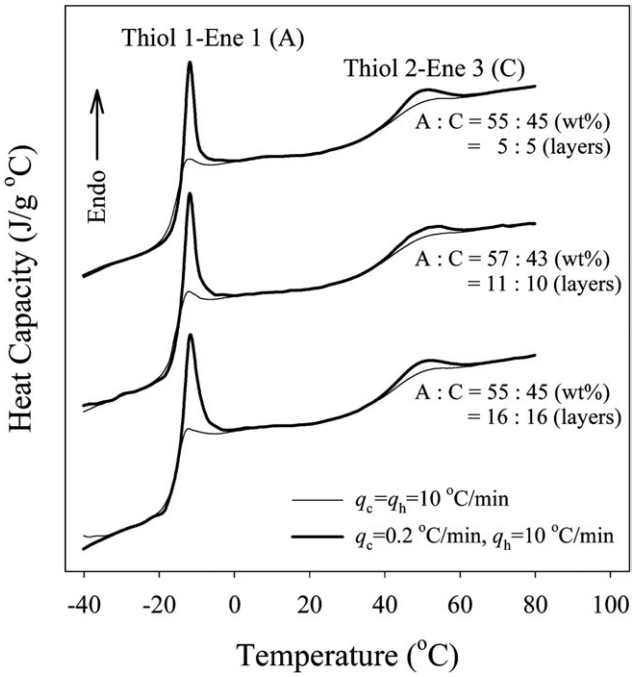

Figure 8. DSC heating scans (q_h = 10 °C/min) of (a) 10-, 21-, and 32-layered thiol-ene network films (set 1, Thiol 1-Ene 1, and Thiol 2-Ene 3) after different cooling rate (q_c = 10 and 0.2°C/min).

Enthalpy Relaxation

Figure 7 shows DSC heating scans of 10- (set 1) and 32-layered (set 2) thiol-ene network films after cooling at different rates (q_c = 10°C/min and 0.2°C/min) as described in Figures 3(a) and 4(a). Differential cooling rate methodology was used to define the distribution and extent of enthalpy relaxation for 10- and 32-layered thiol-ene films independent to the annealing time and temperature dependency on the enthalpy relaxation. For both 10- and 32-layered thiol-ene films, the endothermic peaks by enthalpy relaxation of each layer were observed at its T_g region. The area of enthalpy relaxation produced by differential cooling rate for 10-layered films shows that the layers of Thiol 1-Ene 1 present greater endothermic peak by enthalpy relaxation than Thiol 2-Ene 3 layers [Figure 7(a)] even though the weight ratio of two components are almost the same (55:45). As stated in experimental section, it is due to the different enthalpy relaxation rate of each layer component, which is influenced by chemical structure and can be correlated with the heat capacity change at T_g (ΔC_p). In our previous study, we systematically investigated the effect of chemical parameters of thiol-ene networks such as network density and rigidity on enthalpy relaxation.[15] The higher network density and more rigid chemical structure of thiol-ene networks result in the slower/less extent of enthalpy relaxation as well as smaller ΔC_p. For 32-layered (set 2) thiol-ene network film, the layer number and weight ratio of three network components were quantitatively determined based on the characteristic ΔC_p (Thiol 1-Ene 1 : 0.4985, Thiol 2-Ene 2 : 0.3633, and Thiol 2- Ene 3 : 0.2514 J/g°C) of each component as in bulk resulting in the similar enthalpy relaxation peak area with the ratio of 9:10:13 by layers and 25:35:40 by weight [Figure 7(b)]. In Figure 8, the effect of overall thickness/number of layers with the same thiol-ene layer components on the enthalpy relaxation using set 1 (10-, 21-, and 32-layered thiol-ene network films) is shown. The characteristic enthalpy relaxation peaks by Thiol 1-Ene 1 and Thiol 2-Ene 3 are almost identical, which is due to that each thiol-ene network layer does not affect the molecular mobility of adjacent thiol-ene network layers resulting in independency of enthalpy relaxation behavior to the number of layers/overall thickness of multilayered thiol-ene network films. It is concluded that multilayered thiol-ene films exhibit enthalpy relaxation over wide temperature range due to the different T_gs of each layer as well as the inconsistent enthalpy relaxation will be occurred in a film at a specific annealing condition, i.e. annealing time (t_a) and temperature (T_a). As a result, there are potential problems due to the inconsistency of enthalpy relaxation among layers since each layer has different chemical structure and resultant relaxation times,

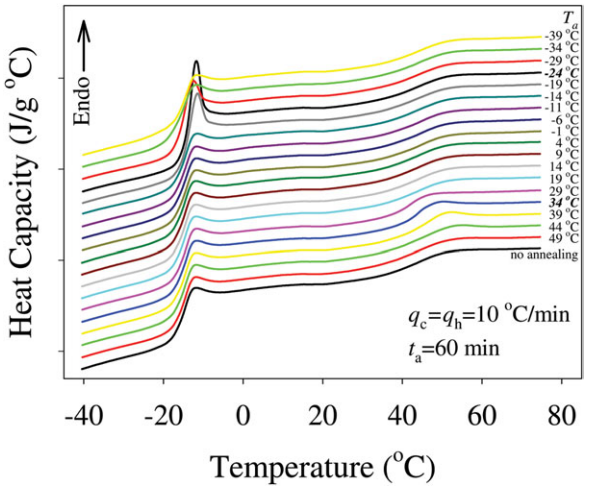

Figure 9. DSC heating scans of the 10-layered thiol-ene film (set 1, Thiol 1-Ene 1, and Thiol 2-Ene 3) after annealing for 1h (t_a = constant) at different temperature (T_a). [Color figure can be viewed in the online issue, which is available at wileyonlinelibrary.com.]

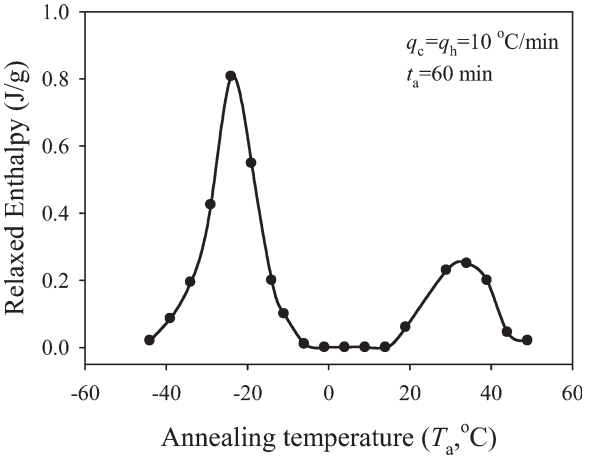

Figure 10. The distribution of enthalpy relaxation of the 10-layered thiol-ene film (set 1, Thiol 1-Ene 1, and Thiol 2-Ene 3) obtained by isochronal aging method (annealing time, t_a = constant, 1 h).

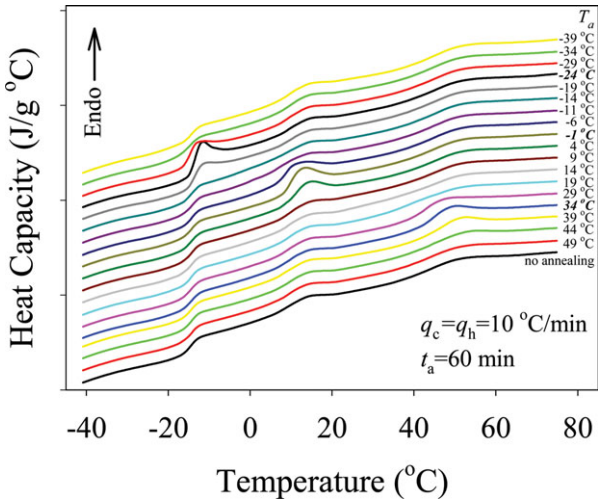

Figure 11. DSC heating scans of the 32- layered thiol-ene film (set 2, Thiol 1-Ene 1, Thiol 2-Ene 2, and Thiol 2-Ene 3) after annealing for 1 h (t_a = constant) at different temperature (T_a). [Color figure can be viewed in the online issue, which is available at wileyonlinelibrary.com.]

which could be a potential problem in physical and mechanical properties of multilayered thiol-ene films.

In Figures 9–12, the temperature dependency of the enthalpy relaxation for both 10- (set 1) and 32-layered (set 2) thiol-ene films is shown. DSC heating scans of 10-layered thiol-ene film after annealing at different temperature from −39 to 49°C for 1h in Figure 9 show that the enthalpy relaxation is clearly temperature dependent. The endothermic peaks due to the enthalpy relaxation are maximum at T_g-10°C of two different components (−24°C for Thiol 1-Ene 1 and 35°C for Thiol 2-Ene 3) and decrease as T_a is getting farther from T_g. This temperature dependency of enthalpy relaxation is affected by two factors such as chain mobility and thermodynamic driving force, and maximum at T_g-10°C is the resultant temperature of the competition of them.[15,16] In general, chain mobility is extremely restricted below T_g-30°C and there is no relaxation over T_g+5 °C because liquid or rubbery state is already thermodynamic equilibrium. Therefore, no enthalpy relaxation was observed from −1∼14°C where temperature is too low for Thiol 2-Ene 3 to be relaxed and it is equilibrium for Thiol 1-Ene 1. Figure 10 shows the distribution of enthalpy relaxation as a function of temperature, which was calculated by the integration of enthalpy relaxation peak as following equation.

$$\Delta H_r(T_a,\ t_a) = \int_{T_g-50^oC}^{T_g+50^oC} C_p(T_a,\ t_a)dT - \int_{T_g-50^oC}^{T_g+50^oC} C_p(T_a,\ 0)dT, \quad (1)$$

where C_p (T_a, t_a) and C_p (T_a, 0) represent specific heat capacities for samples annealed at T_a for $t = t_a$ and unannealed samples, respectively.

For 32-layered (set 2) thiol-ene films, three different thiol-ene layer components showing different glass transition temperature (Thiol 1-Ene 1: T_g = −14°C, Thiol 2-Ene 2: T_g = 10°C, and Thiol 2-Ene 3 : T_g = 45°C) were stacked, which results in three separated T_gs and endothermic peaks due to the enthalpy relaxation. In Figure 11, three different enthalpy relaxation peaks were observed and all of them have maximum at T_g-10°C of each component indicating each layer is independent to adjacent layers. The distribution of enthalpy relaxation as a function of T_a in Figure 12 shows overlapped three peaks corresponding temperature dependency of each component (Thiol 1-Ene 1, Thiol 2-Ene 2, and Thiol 2-Ene from left to right).

The time dependency of enthalpy relaxation for 32-layered (set 2) thiol-ene film characterized by isothermal aging method as described in Figures 3(c) and 4(c) is shown in Figure 13. The 32-layered thiol-ene film was annealed at three different temperatures (-24, -1, and 34°C), where the enthalpy relaxation showed maxima in isochronal aging method, as a function of annealing time (t_a). At each T_a, the extent of enthalpy relaxation increases as increasing t_a at the corresponding T_g region of each layer component but no relaxation was observed at the region of the other two layer components, indicating that the enthalpy relaxation of layers are independent each other. In Figure 14, the extent of enthalpy relaxation (δ_H) of 32-layered thiol-ene film calculated by eq. (1), normalized values by weight ratio of each layer component (Thiol 1-Ene 1 : Thiol 2-Ene 2 : Thiol 2-Ene 3 = 25 : 35 : 40), and that of bulk samples are plotted as a function of logarithmic annealing time. The calculated values are summarized in Table I. To quantitatively analyze the general overall relaxation rate (β_H), a simple eq. (2)[32–36] was applied to the plots in Figure 14.

$$\beta_H = \frac{d\delta_H}{d\log t_a} \quad (2)$$

It is clear that the β_H values obtained from the extent of enthalpy relaxation (δ_H) vs. logarithmic annealing time (t_a) at each T_a in Figure 13 smaller than β_H of bulk samples due to the weight ratio of each layer component in 32-layered (set 2) film. However, the normalized δ_H per unit weight of each layer component is

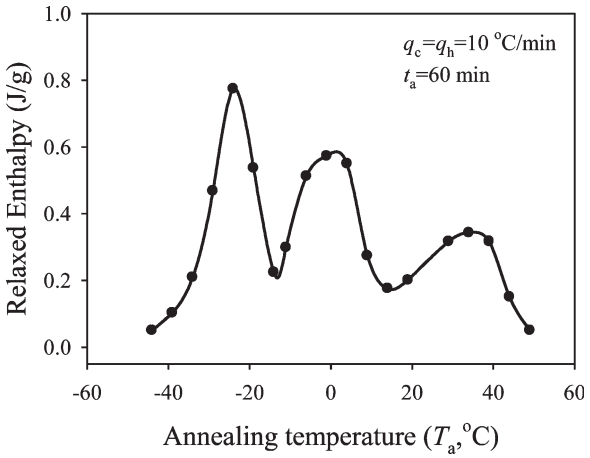

Figure 12. The distribution of enthalpy relaxation of the 32-layered thiol-ene film (set 2, Thiol 1-Ene 1, Thiol 2-Ene 2, and Thiol 2-Ene 3) obtained by isochronal aging method (annealing time, t_a = constant, 1 h).

Applied Polymer SCIENCE

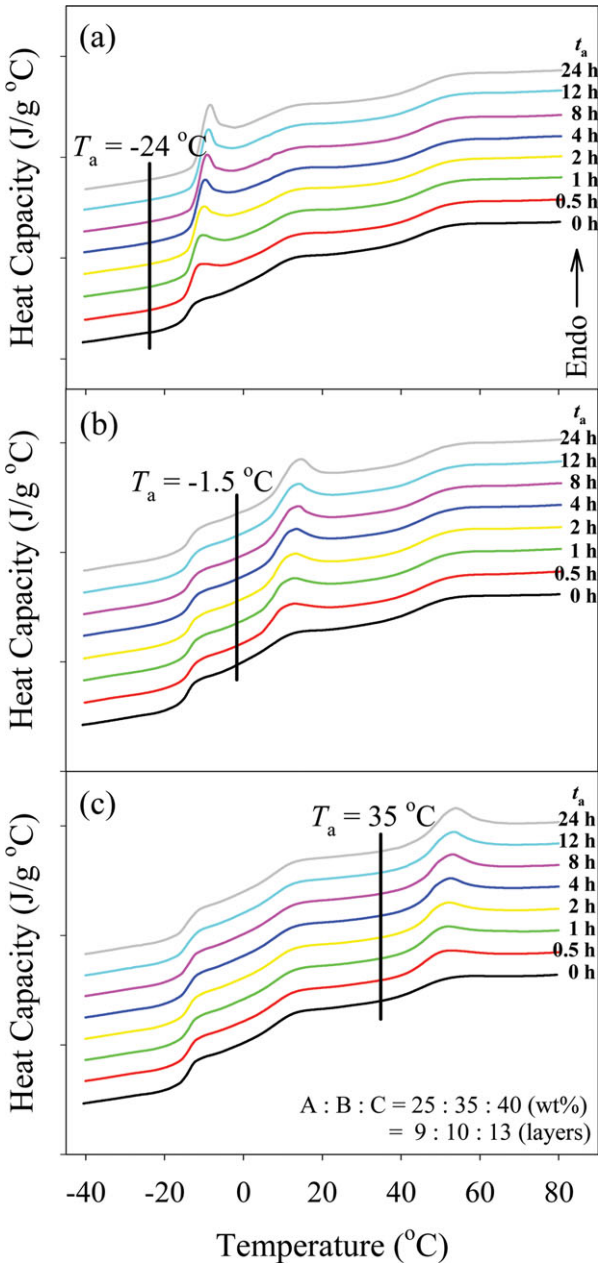

Figure 13. DSC heating scans of the 32-layered thiol-ene film (set 2, Thiol 1-Ene 1, Thiol 2-Ene 2, and Thiol 2-Ene 3) after annealing at three different annealing temperatures (T_a = −24, −1.5, and 35°C) as a function of annealing time. [Color figure can be viewed in the online issue, which is available at wileyonlinelibrary.com.]

considerably greater than δ_H of bulk samples resulting in faster overall relaxation rate (β_H). It is concluded that the thin layers within 32-layered (set 2) film that are not chemically bonded exhibit accelerated enthalpy relaxation compared with that of bulk samples because segmental chain mobility of each layer increases and each layer does not affect each other.

Dynamic Mechanical Thermal Properties

In Figure 15, tan δ and loss modulus of 10- (set 1) and 32-layered (set 2) thiol-ene films are shown. Two and three distinctive transition peaks are observed at T_g of each layer component that is consistent with DSC results. Thus, for 32-layered thiol-ene film, glass transition regions of three different layer components are overlapped and ranges from −20∼80°C. Based on the viscoelasticity, the damping property of a polymer can be estimated by the intensity and area of tan δ or loss modulus (E'').[37] Therefore, it has been reported that thiol-ene networks are a good candidate for high energy absorbing materials due to the high tan δ peak resulted by the highly dense and uniform chemical structure.[1,38–40] However, the narrow glass transition range of thiol-ene resulted by the highly dense and uniform network structure limits energy damping temperature, i.e. working temperature. Consequently, layering thiol-ene films exhibiting high and broad loss modulus (E'') and tan δ as shown in Figure

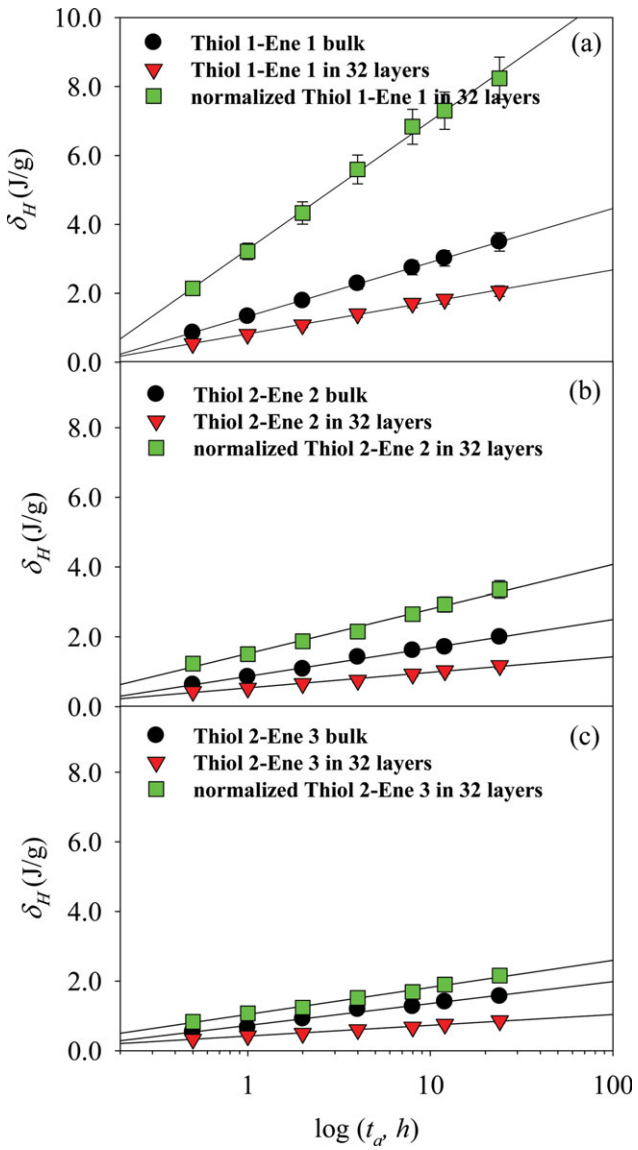

Figure 14. The overall relaxation rates (β_H) of 32 layered thiol-ene film (set 2, Thiol 1-Ene 1, Thiol 2-Ene 2, and Thiol 2-Ene 3) at three different annealing temperatures (T_a = −24, −1.5, and 35°C). [Color figure can be viewed in the online issue, which is available at wileyonlinelibrary.com.]

Table I. The Extents of Enthalpy Relaxation at 24 h (ΔH_{24h}) and Overall Relaxation Rates (β_H) for Three Thiol-Ene Network Components for 10- (set 1, Thiol 1-Ene 1, and Thiol 2-Ene 3) and 32-Layered (set 2, Thiol 1-Ene 1, Thiol 2-Ene 2, and Thiol 2-Ene 3) Films

	ΔH_{24h}[a] (J/g)			β_H[b] (J/g per decade)		
Sample #	Bulk	In layers	Normalized	Bulk	In layers	Normalized
Thiol 1+Ene 1	3.7	2.2	8.7	1.5	0.9	3.7
Thiol 1+Ene 2	2.1	1.2	3.5	0.8	0.4	1.3
Thiol 2+Ene 3	1.7	0.9	2.3	0.6	0.3	0.8

[a]The extent of enthalpy relaxation after 24 h at T_g-10°C, [b]The overall enthalpy relaxation rate at T_g-10°C.

15 could provide the solution to the existing problems of thiol-ene-based materials as energy damping applications.

CONCLUSIONS

10-, 21-, and 32-layered thiol-ene films were successfully prepared by sequentially repeating spin coating and photo-polymerization of two and three different thiol-ene compositions, respectively, to investigate thermal property and enthalpy relaxation behavior of multilayered thiol-ene films. Two and three separated T_gs as well as distinctive enthalpy relaxation peaks were observed for 10-layered (set 1 with Thiol 1-Ene 1 and Thiol 2-Ene3) and 32-layered films (set 2 with Thiol 1-Ene1, Thiol 2-Ene 2, and Thiol 2-Ene 3) as they were in bulk thiol-ene samples indicating that each layer of multilayered thiol-ene network films is independent each other. Isochronal annealing experiments showed temperature dependency of enthalpy relaxation for both 10- (set 1) and 32-layered (set 2) thiol-ene films that are distributed over wide temperature range. Time dependency of enthalpy relaxation for 32-layered (set 2) thiol-ene film was obtained by isothermal annealing experiment at three annealing temperature (T_a) providing the information on the enthalpy relaxation kinetics. The extent (δ_H) as well as overall enthalpy relaxation rate (β_H) was significantly accelerated by layering of thin films compared with bulk samples. Consequently, the enthalpy relaxation of each layer component occur independently at a different temperature, so as a result the inconsistency in physical and mechanical property changes between layers by enthalpy relaxation could be a potential problem to affect the original performance of multilayered thiol-ene films. In other words, the acceleration of enthalpy relaxation by the formation of multilayered thin films is another parameter that has to be considered when designing thiol-ene films.

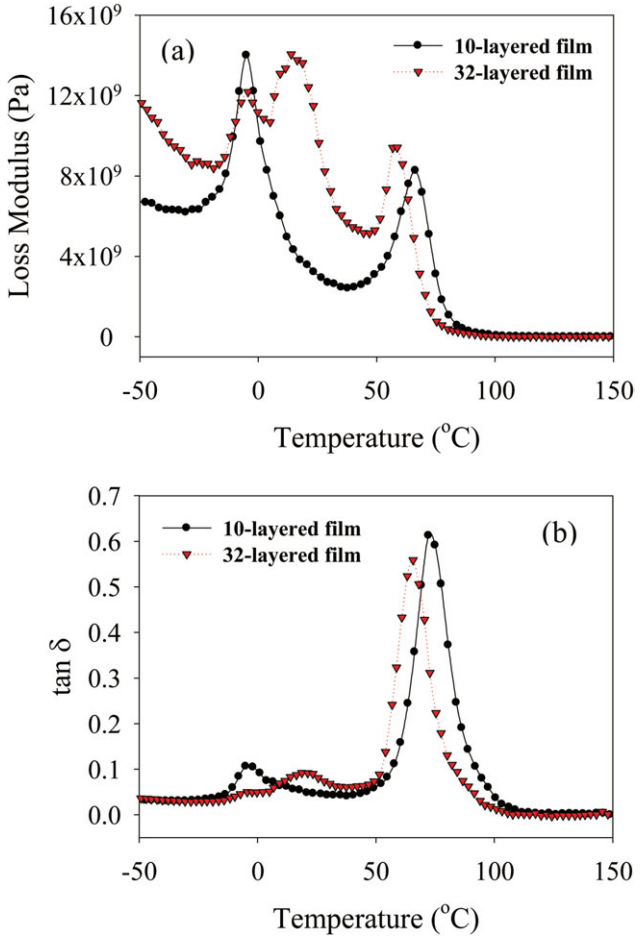

Figure 15. Loss modulus (E'') and tanδ of (a) 10- (set 1, Thiol 1-Ene 1, and Thiol 2-Ene 3) and (b) 32-layered (set 2, Thiol 1-Ene 1, Thiol 2-Ene 2, and Thiol 2-Ene 3) thiol-ene network films. [Color figure can be viewed in the online issue, which is available at wileyonlinelibrary.com.]

Loss modulus (E'') and tan δ of 10- (set 1) and 32-layered (set 2) thiol-ene film showed two and three distinctive peaks corresponding to T_gs of different thiol-ene layer components defined by DSC. For 32-layered thiol-ene film consisting of three different components, glass transition and damping regions are overlapped and the width is extended over 100°C. It is proposed that multilayered structure using thiol-ene exhibiting high damping factor (tan δ) could be a good candidate for an energy damping material in many applications.

Finally, this article mainly discussed about thermal properties and characteristic enthalpy relaxation behavior of thiol-ene network films as in multilayered structure. However, the thickness variation of each layer within the multilayered thiol-ene network films and its resultant effects on physical properties, i.e. glass transition temperature, refractive index, gas permeability, and enthalpy relaxation, are also very interesting topics when especially the size does down to the nanoscale (<100 nm). Thus, "the scale effect" of thiol-ene networks in several different areas is under extensive investigation. In addition, actual energy damping properties such as impact, acoustic, and vibrational damping of multilayered thiol-ene films will be reported in near future.

The authors dedicate this article to the late Dr. Charles E. Hoyle who passed during the preparation of the publication. This article is a small part of his scientific contributions to thiol click chemistry and thiol based polymeric materials. His endeavor and enthusiasm will long be remembered.

ACKNOWLEDGMENTS

The authors also acknowledge Perstorp, Bruno Bock and Ciba Specialty Chemicals for materials, and Fusion UV Systems for the light source.

REFERENCES

1. Hoyle, C. E.; Lee, T. Y.; Roper, T. *J. Polym. Sci. Part A: Polym. Chem.* **2004,** *42*, 5301.
2. Roper, T. M.; Rhudy, K. L.; Chandler, C. M.; Hoyle, C. E.; Guymon, C. A. *RadTech NA Tech. Conf. Proc.* **2002,** 697.
3. Roper, T. M.; Guymon, C. A.; Hoyle, C. E. *Polymer* **2004,** *45*, 2921.
4. Lub, J.; Broer, D. J.; Allan, J. F. *Mol. Cryst. Liq. Cryst. Sci. Tech. Sect. A: Mol. Cryst. Liq. Cryst.* **1999,** *332*, 2769.
5. Toh, H. K.; Chen, F.; Kok, C. M. U.S. Patent 6,172,140, (**2001**).
6. Cramer, N. B.; Scott, J. P.; Bowman, C. N. *Macromolecules* **2002,** *35*, 5361.
7. Cramer, N. B.; Davies, T.; O'Brien, A. K.; Bowman, C. N. *Macromolecules* **2003,** *36*, 4631.
8. Cramer, N. B.; Reddy, S. K.; O'Brien, A. K.; Bowman, C. N. *Macromolecules* **2003,** *36*, 7964.
9. Okay, O.; Reddy, S. K.; Bowman, C. N. *Macromolecules* **2005,** *38*, 4501.
10. Reddy, S. K.; Cramer, N. B.; Bowman, C. N. *Macromolecules* **2006,** *39*, 3673.
11. Senyurt, A. F.; Wei, H.; Hoyle, C. E.; Piland, S. C.; Gould, T. E. *Macromolecules* **2007,** *40*, 4901.
12. Wei, H.; Li, Q.; Ojelade, M.; Madbouly, S.; Otaigbe, J. U.; Hoyle, C. E. *Macromolecules* **2007,** *40*, 8788.
13. Scott, T. F.; Kloxin, C. J.; Draughon, R. B.; Bowman, C. N. *Macromolecules* **2008,** *41*, 2987.
14. Shin, J.; Matsushima, H.; Comer, C. M.; Bowman, C. N.; Hoyle, C. E. *Chem. Mater.* **2010,** *22*, 2625.
15. Shin, J.; Nazarenko, S.; Hoyle, C. E. *Macromolecules* **2008,** *41*, 6741.
16. Shin, J.; Nazarenko, S.; Hoyle, C. E. *Macromolecules* **2009,** *42*, 6549.
17. Frank, C. W.; Rao, V.; Despotopoulou, M. M.; Pease, R. F. W.; Hinsburg, W. D.; Miller, R. D.; Rabolt, J. F. *Science* **1996,** *273*, 912.
18. Pfromm, P. H.; Koros, W. J. *Polymer* **1995,** *36*, 2379.
19. McCaig, M. S.; Paul, D. R. *Polymer* **2000,** *41*, 629.
20. McCaig, M. S.; Paul, D. R.; Barlow, J. W. *Polymer* **2000,** *41*, 639.
21. Kim, J. H.; Jang, J.; Zin, W. C. *Langmuir* **2000,** *16*, 4064.
22. Pham, J. Q.; Green, P. F. *Macromolecules* **2003,** *36*, 1665.
23. Forrest, J. A.; Dalnoki-Veress, K.; Stevens, J. R.; Dutcher, J. R. *Phys. Rev. Lett.* **1996,** *77*, 2002.
24. Keddie, J. L.; Jones, R. A. L.; Cory, R. A. *Faraday Discuss* **1994,** *98*, 219.
25. Wallace, W. E.; van Zanten, J. H.; Wu, W. L. *Phys. Rev. E* **1995,** *32*, R3329.
26. Huang, Y.; Paul, D. R. *Macromolecules* **2006,** *39*, 1554.
27. Dorkenoo, K. D.; Pfromm, P. H. *J. Polym. Sci. Part B: Polym. Phys.* **1999,** *37*, 2239.
28. Pinnau, I.; Koros, W. J. *J. Appl. Polym. Sci.* **1991,** *43*, 1491.
29. Roth, C. B.; Torkelson, J. M.; *Macromolecules* **2007,** *40*, 3328.
30. Weber, M. F.; Stover, C. A.; Gilbert, L. R.; Nevitt, T. J.; Ouderkirk, A. J. *Science* **2000,** *287*, 2451.
31. Leibler, L. *Prog. Polym. Sci.* **2005,** *30*, 898.
32. Hutchinson, J. M. *Prog. Polym. Sci.* **1995,** *20*, 703.
33. Pan, P.; Zhu, B.; Inoue, Y. *Macromolecules* **2007,** *40*, 9664.
34. Ju, H.; Nutt, S. *Macromolecules* **2003,** *36*, 4010.
35. Struik, L. C. E. *Polymer* **1987,** *28*, 1869.
36. Struik, L. C. E. Physical Aging in Amorphous Polymers and Other Materials, Elsevier Publishing Company: New York, **1978.**
37. Klempner, D.; Sperling, L. H.; Utracki, L. A. Advances in Chemistry Series 239: Interpenetrating Polymer Networks; ACS, New York, **1991.**
38. Senyurt, A. F.; Wei, H.; Phillips, B.; Cole, M.; Nazarenko, S.; Hoyle, C. E.; Piland, S. G.; Gould, T. E. *Macromolecules* **2006,** *39*, 6315.
39. Senyurt, A. F.; Wei, H.; Hoyle, C. E.; Piland, S. G.; Gould, T. E. *Macromolecules* **2007,** *40*, 4901.
40. Senyurt, A. F.; Wei, H.; Hoyle, C. E.; Piland, S. G.; Gould, T. E. *Macromolecules* **2007,** *40*, 3174.